Chemistry Africa (2023) 6:1335–1347
https://doi.org/10.1007/s42250-022-00565-4

ORIGINAL ARTICLE

Identification of Phyto-Compounds from *Ilex kudingcha* as Inhibitors of Sterol-14α-Demethylase Protease: A Computational Approach Against Chagas Disease

Damilola A. Omoboyowa[1] · Jamiu A. Kareem[1] · Oluwatosin A. Saibu[2] · Damilola S. Bodun[1] · Temitope M. Ajayi[3] · Oluwatoba E. Oyeneyin[4]

Received: 3 October 2022 / Accepted: 5 December 2022 / Published online: 20 December 2022

Abstract
Trypanosoma cruzi causes chagas disease, a life threating disease in non-endemic and endemic regions globally, the life cycle of *T. cruzi* strictly depends on endogenous synthesis of sterol via 14-α-demethylase pathway. The available drugs for chagas disease treatment are currently resistance and parade unwanted side effects. Herein, molecular docking, QSAR, molecular mechanics/generalized born surface area (MM/GBSA) estimation, ADME screening, and molecular dynamics (MD) simulation were performed using Schrodinger suite to identify 14-α-demethylase protease antagonist from *Ilex kudingcha*. Density function theory of the hit ligands was carried out using Spartan 14 to investigate the molecular reactivity of the lead molecules. Nine (9) hit molecules were predicted as 14-α-demethylase protease inhibitors with binding energy range of −7.632 to −9.559 kcal/mol which was comparable to the standard drug (benznidazole = −6.969), two lead molecules were further subjected to MD simulation over 50 ns predicting that kulactone and gallocatechin form stable interactions with vital residues at the catalytic site of the protein. DFT analysis revealed that, the hit ligands have the ability to donate and accept proton donating and accepting hence, effective as solubility and inhibitory agent and the ADME screening revealed, all the hit ligands obey Lipinski rule of five presenting them as drug candidate. The observations from this study predict kulactone and gallocatechin as putative antagonist of 14-α-demethylase protease and should be experimentally verify as a lead compound for chagas disease therapy.

Keywords *Ilex kudingcha* · Chagas disease · Computational models · Phyto-compounds

1 Introduction

Chagas disease (CD) common known as American trypanosomiasis is one of the neglected tropical diseases (NTDs) caused by *Trypanosoma cruzi*, this protozoan is spread by kissing bug [1], the disease constitute one of the serious public health issues in most endemic countries [2]. The World Health Organization (WHO) reported that almost 6–7 million individuals globally are victim of CD. It is common in the rural areas of Latin American nations, where it is contacted by humans and other mammals through contact with the waste or urine of kissing bug (triatomine bugs) [3]. The disease has spread beyond the Latin American nations due to migration from these endemic countries to Japan, the United States, Canada, and Australia [4].

Contact with *T. cruzi*, the host is permanently infected with chagas disease which has three (3) stages: acute, indeterminate, and chronic [5]. The acute stage of chagas disease occurs immediately after infection, and the symptoms are difficult to detect due to the relatively non-specific clinical symptoms observed in the majority of infected patients, as well as the ancient and subjective methods available [6].

✉ Damilola A. Omoboyowa
damilola.omoboyowa@aaua.edu.ng

[1] Department of Biochemistry, Adekunle Ajasin University, Akungba-Akoko, Ondo State, Nigeria

[2] Department of Environmental Toxicology, Universitat Duisburg-Essen, Duisburg, North Rhine-Westphalia, Germany

[3] Department of Biochemistry, Ladoke Akintola University of Technology, Ogbomoso, Oyo State, Nigeria

[4] Theoretical and Computational Chemistry Unit, Department of Chemistry, Adekunle Ajasin University, Akungba-Akoko, Ondo State, Nigeria

This delay in diagnosis has an impact on the infected by impeding treatment and thus the cure [7].

nifurtimox and Benznidazole have been the initial-line treatments for CD for many years. CD regarded as a neglected disease, therefore there is lack of competition among drug manufacturers to meet production quality criteria. It is also worth noting that the current and only CD medications are prohibitively expensive, making them inaccessible to CD patients [8]. Production of sterols by 14-α-demethylase is a vital pathway in the life cycle of *T. cruzi* [1]; sterol 14-α-demethylase protease is in charge of mammalian cholesterol biosynthesis. *T. cruzi* wholly relay on biologically active sterols for proliferation and survival, they cannot use host cholesterol; therefore, the parasite's sterol biosynthetic pathway is particularly appealing for drug development [9].

The unique biochemical activities and health benefits of phytochemicals pre-dates to human existence and most of the available pharmaceuticals are isolated from medicinal plants which have proven to possess herbal remedies [10]. Ilex, commonly known as holly, belongs to the family aquifoliaceae. Kudingcha, a bitter spike tea from *Ilex latifolia* and *Ilex kudingcha* is taken as a medicinal herb in southern China. Kudingcha is referred to as a dietetic drink and is becoming well-known with trade names green-golden tea, beauty-slimming tea, clearing-heat tea and longevity tea in China. *Ilex kudingcha* has been observed to possess anti-inflammatory, lipid metabolism, antioxidant and anti-tumor properties [11, 12]. Soniran et al., [13] has reported the in vitro anti-trypanosomal activities of methanol and chloroform extracts of *Ilex kudingcha* with their effects on the hepatocytes. The anti-trypanosomal mechanisms of the phyto-compounds from *Ilex kudingcha* have not been studied. Therefore, we aim to explore computational approaches to predict inhibitory activities of phyto-compounds from *Ilex kudingcha* against *T. cruzi* 14-*α*-demethylase protease.

2 Materials and Methods

2.1 Ligands and Protein Structure Preparation

Ninety-eight (98) compounds from *Ilex kudingcha* gotten from literature search were retrieved from database of PubChem (https://pubchem.ncbi.nlm.nih.gov), the compounds were prepared by Ligprep tool from Schrodinger suite according to Omoboyowa [14].

The crystallographic structure of sterol-14α-demethylase protease was downloaded from databank (pdb: 4CKA) (https://www.rcsb.org/). This biomolecule was prepared with protein preparation wizard to rectify all errors including assigning of bond orders and missing hydrogen atoms. Receptor grid generation tool was used to generate the target glide grid file at the binding site of the co-crystalized ligand which automatically generate coordinates x = 0.52, y = 26.38, z = 459.97.

2.2 Quantum Chemical Calculation

The lead molecules were minimized by the DFT/Becke Three Lee Yang Parr/6-31G(d) level of theory, restricted hybrid Hartree Fock-DFT self-consistent field calculation with Pulay's direct inversion of the iterative sub-space and geometric direct minimization was employed using Spartan 14 computational chemistry software. The HOMO and LUMO energies (E_{HOMO} and E_{LUMO}) were calculated with the reactivity descriptors extrapolated from the E_{HOMO} and E_{LUMO} values [15].

2.3 Virtual Screening by Molecular Docking

Ninety-eight (98) ligands from *I. kudingcha* and reference drug (Benznidazole) were screened through HTVS docking precision. Twenty (20.4%) of the lead ligands were further screened by SP and XP docking precision, the top-scored ligands with higher docking score than the reference drug were finally selected. Validation of the screening protocol was carried out by extracting, preparing and re-docking of the co-crystalized ligand into the original catalytic site of 4CKA to validate the reliability of the docking procedure [14].

2.4 Calculation of the MM/GBSA

The docked ligands-sterol-14α-demethylase protease complexes were optimized by local optimization feature in prime, binding energies (Δ^{bind}) for the ligands-sterol-14α-demethylase protease complexes were determined by the OPLS3 force field. The MM/GBSA estimation was performed on the docked complexes using the formula:

$$\Delta G^{bind} = \Delta E^{MM} + \Delta G^{solv} + \Delta G^{SA}$$

2.5 Screening for ADME Profile

The pharmacokinetic and drug-likeness profile of the lead ligands from *I.kudingcha* was predicted by the Qikprop tool of Schrodinger suite.

2.6 Development of Automated QSAR Model

The experimental data with pIC_{50} of 14α-demethylase protease antagonists were retrieved from the database of CHEMBL via www.ebi.ac.uk/chembl/ by blasting of the protein FASTA sequence. The inhibitors were converted

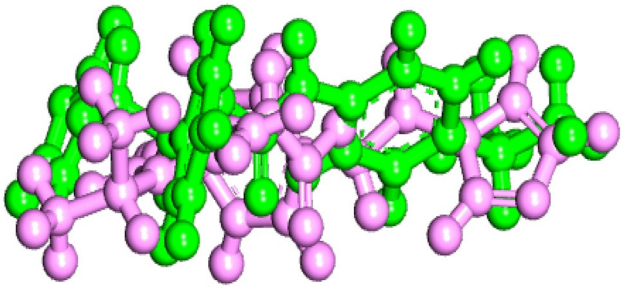

Fig. 1: 4CKA co-crystalized ligand overlapped at its binding domain

to sdf format using DataWarrior v.2 [1]. The file saved as sdf was uploaded onto the workspace of the software and prepared by macromodel minimization. QSAR model for 14α-demethylase protease was developed based on the inhibitors' pIC_{50}. Mlr_2 model was preferred based on the ranking outcomes.

2.7 Molecular Dynamic Simulation

Molecular dynamics simulation tends to compute the movement of atoms based on time by incorporating the classical equation of Newton's motion. The simulations were performed for a period of 50 ns with Desmond tool of Schrödinger suite. The ligand–protein docking complexes were the initial stages of the simulation; this was carried out to determine the binding status of the ligands in physiological state.

The pre-process of the protein–ligand complexes were performed using protein preparation wizard of Schrodinger suite which involve the minimization and optimization of complexes. All systems were prepared by the System Builder tool according to the protocol described by Omoboyowa et al. [15].

3 Results and Discussion

3.1 Post-Docking Analysis and Calculation of MM/GBSA

Molecular docking remains an important and established computational structural based virtual screening method employed in drug discovery and design. It predicts potential drug targets and molecular ligand-target interactions at the atomic level [16]. In this study, the molecular docking protocol was validated by preparation of extracted co-crystalized ligand, re-docked it into the active site of the target. Figure 1 represents the overlapping of the re-docked ligand, the ligand deviated from its original geometry with RMSD value of 0.74 Å (> 2.0 Å), suggesting the reproducibility and reliability of the protocol [17].

The binding affinity of the nine (9) lead molecules and the standard drug (structures shown on figure S1) are presented in Fig. 2, the result reveals that, the nine hit compounds have higher binding affinity compared with the standard drug (benznidazole) (− 6.979 kcal/mol). Kulactone showed the highest binding affinity of − 9.559 kcal/mol at the binding domain of the target, since the negativity of the binding energy reveal the intensity of the interaction [15]. Molecular docking has been reported to form a key method used in the drug discovery process. The pharmaceutical industries

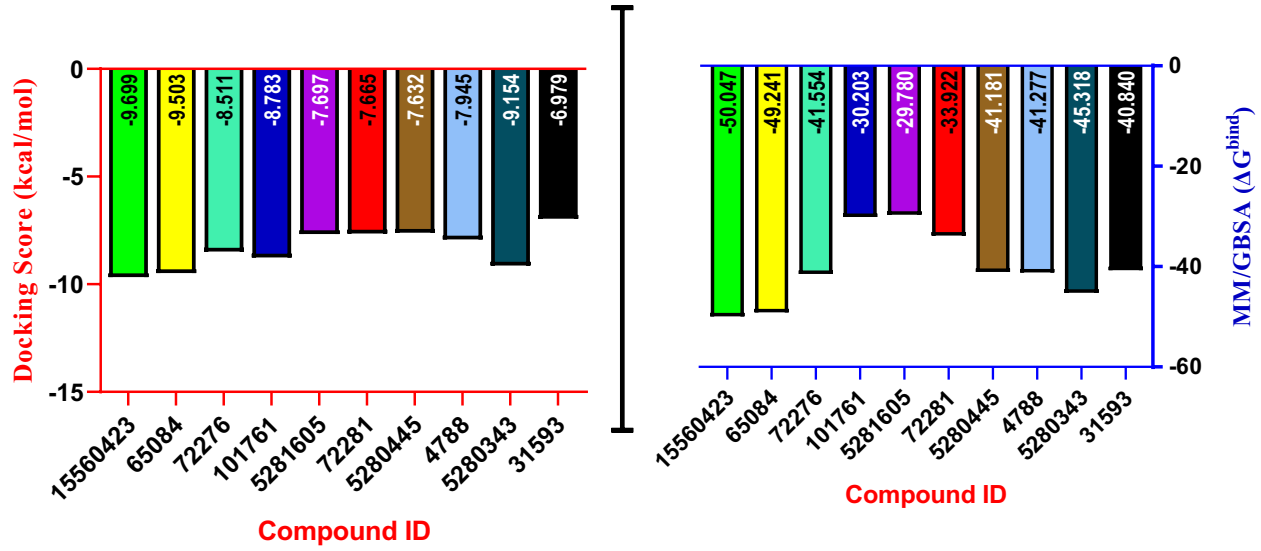

Fig. 2 Representation of the binding affinity and MM/GBSA (ΔG^{bind}) of lead compounds viz: 15560423: Kulactone; 65084: (+)(−)Gallocatechin; 72276: (−)(−)Epicatechin; 101761: Erythrodiol; 5281605: Baicalein; 72281: Hesperetin; 5280445: Luteolin; 4788: Phloretin; 5280343: Quercetin; 31593: Benznidazole

Table 1 Post docking analysis of the docked complexes

Compound name	No H-bonds	Interacting amino acid
Kulactone	1	CYS 422
(+)(−)Gallocatechin	2	CYS 422; TYR 103
(−)(−)Epicatechin	3	TYR 116; MET 358
Erythrodiol	1	CYS 422
Baicalein	2	CYS 422; TYR 103
Hesperetin	1	CYS 422
Luteolin	3	TYR 166; MET 460; LEU 357
Phloretin	2	MET 460; TYR 116
Quercetin	3	ALA 291; MET 358
Benznidazole (standard)	2	TYR 116

currently rely on this computational model to screen large library of compounds to identify novel molecules for design of new therapeutic agent [18]. From Table 1 and Fig. 3, (−)(−)epicatechin, Luteolin and Quercetin showed three H-bonds interaction with the residues at the binding domain of the protein while the standard drug (benznidazole) showed 2 H-bonds interaction with TYR 116. The interaction of small molecules with the catalytic site amino acid of protein is necessary for their inhibitory activity [1]. Five hit compounds were observed from Table 1 to form H-bond with CYS 422. Cysteine (CYS) has been observed to act as a switch to control the activity of proteins including metabolic enzymes, transcription factors and protein kinases [19, 20]. Thus, the functional importance and high nucleophilicity and of CYS makes it attractive for development of targeted covalent ligands to modulate the function of diverse proteins [21].

The MM/GBSA protocol is a popular model to calculate the binding free energy of small ligands binding to biological macromolecules. They are intermediate in accuracy and computational effort of strict alchemical perturbation methods and empirical scoring, which have been applied to a large number of systems with varying degree of success [22]. Herein, the free binding energy values (Δ^{bind}) of the hit compounds-protein complexes were presented in Fig. 2, the result reveals that, kulactone (− 50.047) has the highest negative value for the MM/GBSA. Erythrodiol (− 30.203), baicalein (− 29.783) and hesperetin (33.933) were observed to have lower negative MM/GBSA values compared with the standard drug (− 40.840), with other compounds presenting higher negative values than the standard drug.

3.2 Pharmacokinetics and Drug-Likeness Screening

Pharmacokinetic profiling relate to the metabolism and excretion of drug candidates. These features are predicted after drug discovery protocol; however, with computational tools such absorption, distribution, metabolism and excretion (ADME) profiles can be carried out at the early stage of drug design. Optimization of the ADME profiles of small molecules is often the most challenging part of drug discovery process which also has a major impact on the probability of success of drug candidates [23]. Herein, the nine (9) top-scored compounds from the post-docking analysis were screened for their ADME properties. From Table 2, Lipinki's rule of five was use to predict the drug likeness of the compounds which includes H-bond donor (> 5.00), H-bond acceptor (> 10), and molecular weight (> 500 KD) [24]. Interesting, the entire lead compound obeyed Lipinski rule of five with at most one violation, this suggest that the lead compounds are drug candidates.

The pharmacokinetic profiles of the hit compounds were analyzed for QPP^{caco}, $QPlog^{HERG}$, QPP^{MDCK}, $QPlog^{BB}$, $QPlog^{kp}$ and $QPlog^{khsa}$ parameters using Qikprop of Schrodinger suite. From Table 3, the result showed that, the hit ligands are within the recommended range for brain/blood partition coefficient (− 1.3 to 1.2) and the IC_{50} $QPlog^{HERG}$ (> − 5). The results obtained reveal that the hit ligands have low $QPlog^{HERG}$ values suggesting that, the hit compounds could block hERG channels therefore more cardiotoxic [25]. Penetration of the blood–brain barrier is often reported as a significant barrier in the neurological drug development stages [26]. This has been reported to obstruct the entry of drug molecules into the central nervous system (CNS), hence poses as a serious challenge in drug discovery for the CNS disorders [1]. Only kulactone and erythrodiol showed great calcium carbonate (Caco) cell permeability of 1507.214 nm/s and 1905.837 nm/s respectively observed to be greater than the reference value of 25 nm/s. The Caco cell line is use as a model of human intestinal absorption of new therapeutic agents [27]. The Madin-Darby Canine kidney (MDCK) cells are used for the rate of drug active transport, permeability and efflux in drug design [28]. (+)(−)Gallocatechin (6.689 nm/s) and Quercetin (7.210 nm/s) were observed with low QPP^{MDCK} values.

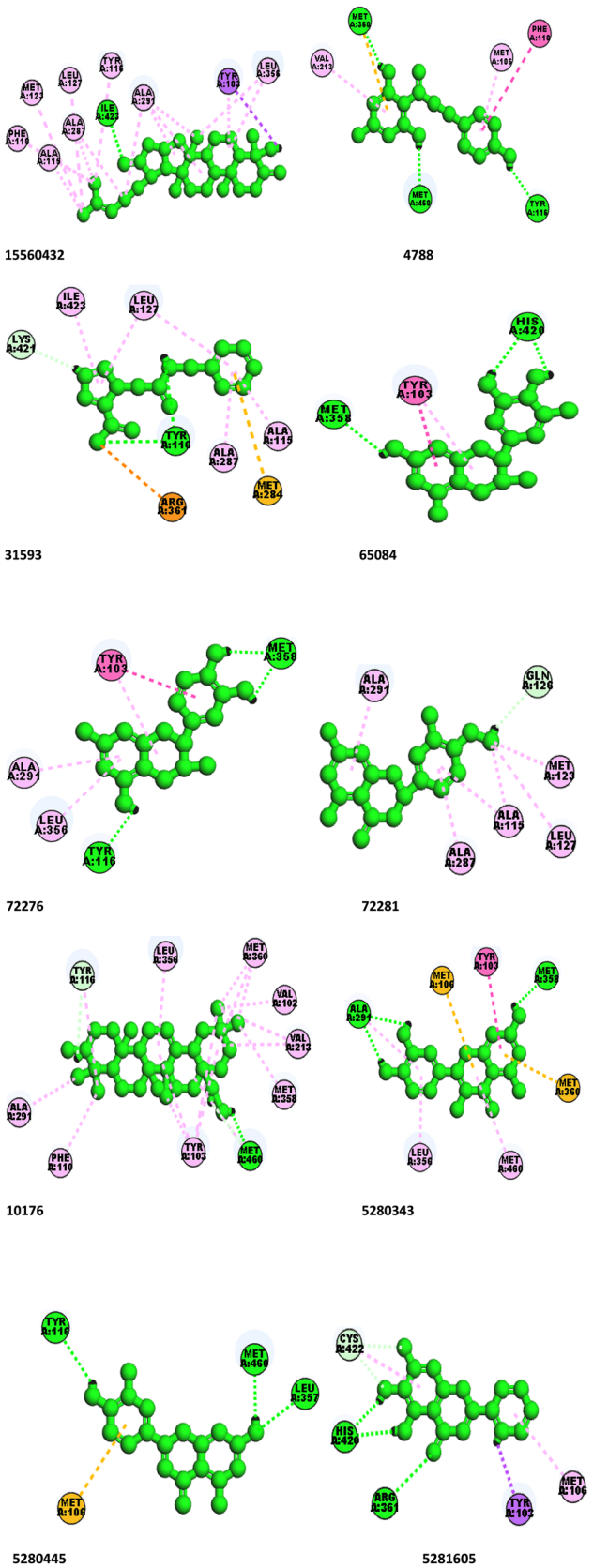

Fig. 3 2D interaction of lead molecules at the binding domain of 14α-demethylase viz: 15560423: Kulactone; 65084: (+)(−)Gallocatechin; 72276: (−)(−)Epicatechin; 101761: Erythrodiol; 5281605: Baicalein; 72281: Hesperetin; 5280445: Luteolin; 4788: Phloretin; 5280343: Quercetin; 31593: Benznidazole

3.3 Analysis of Auto QSAR Model

Quantitative structure–activity relationship (QSAR) is vital tool in computational model that reveals the connection between chemical molecules and structural features [29]. AutoQSAR is a plugin in Schrodinger suite with various topological descriptors with independent variable for generation of models [1]. From Table 4, the autoQSAR splits the dataset into 23% test and 77% train set as computed from the predictive model (mrl_2) for the experimental data. The parameters generated from the model includes: standard deviation (S.D) (0.7123), R^2 (0.5265), root mean square error (RMSE) (0.6855) and the predictive squared correlation coefficient (Q^2) (0.5202) as shown in Table 5. Figure 4 showed the scatter plot of the observed activity and predicted activity of the dataset which revealed more train set (blue colour) than the test set (red colour). The result on the plot was consistent with the data on Table 4. The inhibitory capacity (pIC_{50}) of the lead molecules and reference ligand were predicted base on the generated best predictive model is presented in Table 6. IC_{50} is the half maximal inhibitory concentration of an inhibitor required for 50% inhibition of proteins *in-vitro* [30]. All the hit compounds were observed to posess lower PIC_{50} values compared with the standard drug.

3.4 Density Functional Theory Analysis

Density functional theory (DFT) has been estimated through quantum mechanical methods and showed competence to be employed in pharmacological studies. Hence, DFT has formed a vital protocol in drug designing process [31]. The energies of highest occupied molecular orbital (HOMO) and Least unoccupied molecular orbital (LUMO) are vital orbital descriptors of small molecules, play vital roles in the electric properties, optical and quantum chemistry [32]. Other descriptors such as energy band gaps (E_g), chemical hardness (η), softness (δ), Electronegativity (χ) and chemical potential (Cp) were obtained from the HOMO and LUMO energies as shown in Table 7.

The E_{HOMO} and E_{LUMO} give reveals the reactivity of the compounds, while E_{HOMO} reveals the electron donating ability of molecules; E_{LUMO} predicts the electron acceptance ability. Hence, the higher the E_{HOMO} the more readily

Table 2 Prediction of drug likeness of lead compounds

Compound ID	Mol MW	HB-acceptor	HB-donor	TPSA	RO5 violation
Kulactone	452.68	5	0	61.5	1
(+)(−)Gallocatechin	306.27	6.2	6	137.5	1
(−)(−)Epicatechin	290.27	5.5	5	114.0	0
Erythrodiol	442.72	3.4	2	39.5	1
Baicalein	270.24	3.7	2	96.5	0
Hesperetin	302.28	4.7	2	106.7	0
Luteolin	286.24	4	3	120.3	0
Phloretin	274.24	3	2	109.9	0
Quercetin	302.24	5.3	4	141.9	0
Benznidazole (standard)	260.25	5	1	94.5	0

[a]Molecular weight (> 500.0)

[b]Number of H-bond donors (> 6.0)

[c]Number of H-bond acceptors (> 10.0)

[d]PSA: (7.0–200.0)

[e]Number of Lipinski's rule violation (> 1)

Table 3 Pharmacokinetic prediction of lead compounds

Compounds	QPlogHERG	QPPCaco	$Qplog^{BB}$	QPPMDCK	QPlogKhsa	% Oral Ab
Kulactone	−4.439	1507.214	−0.454	707.780	1.350	100
(+)(−)Gallocatechin	−4.703	18.657	−2.414	6.689	−5.66	35.404
(−)(−)Epicatechin	−4.619	58.241	−1.815	22.893	−0.423	61.197
Erythrodiol	−3.812	1905.837	−0.290	993.321	1.565	100
Baicalein	−5.136	180.219	−1.247	77.617	−0.051	77.487
Hesperetin	−4.618	171.826	−1.313	73.718	−0.037	77.118
Luteolin	−5.022	45.023	−1.910	17.333	−0.205	62.050
Phloretin	−5.198	76.256	−1.989	30.639	0.019	72.945
Quercetin	−5.035	20.000	−2.352	7.210	−0.354	52.348
Benznidazole (STD)	−3.665	341.442	−0.958	232.305	−5.576	79.370

the molecule donate electrons and the lower the E_{LUMO} the more readily the molecule accept electrons, this predict the reactivity of molecules [32]. From Table 7 and Fig. S2, the value of E_{HOMO} (−5.48 eV and −6.69 eV) showed that the molecules would interact readily through donation of electrom. The E_{LUMO} values (−0.78 eV and −2.76 eV) indicated that the molecules would be an electron acceptor. The standard drug (benznidazole) showed higher E_{HOMO} and E_{LUMO} values (−6.69 and −2.76 respective) compared with the hit compounds, suggesting that the standard would readily donate and accept protons than the hit compounds. The reactivity of the compounds was further ascertained by the values of other descriptors derived from the E_{HOMO} and E_{LUMO} such as chemical hardness, softness, electronegativity and chemical potential (Table 7).

3.5 Molecular Dynamic Simulations of 14-α-Demethylase Protease-Ligand Complexes

The post-docking analysis, QSAR modeling and pharmacokinetic profiles of the lead compounds from *Ilex kudingcha* were carefully studied, kulactone and (+)(−)gallocatechin were observed as potent inhibitors of sterol-14-α-demethylase protease; therefore, to validate the ligands' conformational stability at the binding pocket of the protein, the docked complexes of kulactone, (+)(−)gallocatechin and standard drug

Table 4 Auto-QSAR predicted activities vs observed activities

ID	Set	pIC_{50} (observed)	pIC_{50} (predicted)	Residue error
1	Train	6.9000	5.7334	−1.166
2	Train	4.7000	5.2538	0.5537
3	Train	4.1000	4.8492	0.7492
4	Train	5.2000	4.4527	−0.7473
5	Test	4.5000	4.6417	0.1417
6	Train	6.5000	5.4631	−1.0369
7	Train	5.3000	4.5627	−0.7373
8	Train	4.5000	5.0931	0.5931
9	Test	4.9000	4.4173	−0.4827
10	Test	4.6000	4.0746	−0.5254
11	Train	7.0000	6.6248	−0.3752
12	Test	4.4000	4.7580	0.3580
13	Test	5.0000	4.7970	−0.2030
14	Train	4.9000	4.7936	−0.1064
15	Train	7.0000	6.4020	−0.5980
16	Train	4.1000	5.1142	1.0142
17	Train	4.3000	4.9430	0.6430
18	Train	4.4000	4.6734	0.2739
19	Train	5.0000	4.7995	−0.2005
20	Train	6.7000	6.0401	−0.6599
21	Train	5.3000	4.7511	−0.5489
22	Train	4.3000	4.7012	0.4012
23	Train	6.7000	5.9598	−0.7402
24	Test	5.5000	5.3624	−0.1376
25	Train	5.1000	5.2445	0.1445
26	Train	4.6000	4.4796	−0.1204
27	Train	5.6000	5.4990	−0.1010
28	Test	5.5000	5.4916	−0.0084
29	Train	4.5000	4.9407	−0.1010
30	Train	4.9000	5.9875	1.0875
31	Train	4.8000	5.5838	0.7838
32	Train	7.3000	6.1116	−1.1884
33	Test	5.0000	4.8911	−0.1089
34	Train	7.8000	6.4871	−1.3129
35	Test	4.5000	5.2332	0.7332
36	Train	5.5000	4.5072	−0.9928
37	Train	5.3000	5.1746	−0.1254
38	Test	4.3000	5.2614	0.9614
39	Train	4.2000	5.2071	1.0071
40	Train	4.7000	5.1706	0.4706
41	Test	5.1000	5.4260	0.3246
42	Train	5.0000	5.0524	0.0524
43	Train	4.3000	5.3050	1.0050
44	Train	4.1000	4.4299	0.3299
45	Test	7.6000	6.5842	−1.0158
46	Train	4.9000	4.8016	−0.0984
47	Train	4.5000	4.7830	0.2830
48	Train	4.4000	4.8104	0.4140
49	Train	4.5000	5.1517	0.6517
50	Train	6.0000	5.2851	−0.7149
51	Train	4.8000	5.0783	0.2783
52	Train	5.1000	5.5087	0.4087
53	Train	5.1000	4.7573	−0.3427
54	Train	4.1000	4.9368	0.8368
55	Test	6.9000	5.7637	−1.1363
56	Train	4.5000	4.9713	0.4713
57	Train	4.6000	4.5146	−0.0854
58	Test	6.5000	5.1335	−1.3665
59	Train	6.5000	5.5462	−0.9538
60	Train	4.3000	5.1122	0.8122

Table 5 Parameters for the autoQSAR of the predictive model

Model code	SD	R^2	RMSE	Q^2
kpls_linear_45	0.7123	0.5265	0.6855	0.5202

(benznidazole) with the target were used for 50 ns MD simulation. The docked complex stability is an important factor in studying the inhibitory mechanism of protein from molecular docking protocol [33]. Each compound's root-mean-square fluctuation (RMSF), root-mean-square deviation (RMSD) and hydrogen bond mapping were analyzed. RMSD gives details about the protein concerning its structural backbone [34]. Figure 5 showed the RMSD plot of the target (Cα) and ligands fit protein over 50 ns simulation trajectory for kulactone, gallocatechin and standard drug. The Cα atoms in sterol-14-α-demethylase protease complexes with hit compounds exhibited mean deviation range was observed to be less than 4.0 Å (< 4.0 Å) which is acceptable for small globular proteins. The RMSD of sterol-14-α-demethylase protease and gallocatechin complex showed initial fluctuation between 1.0 and 1.50 Å within the 20 ns of simulation. After 20 ns of simulation, the trajectory was showed to be stable to the end of the simulation time. The RMSD of kulactone and sterol-14-α-demethylase protease complex showed stability for the first 10 ns of simulation with slight fluctuation of 1.5–2.1 Å differences. Between 10 and 20 ns, there was significant large difference in the RMSD value of Cα and Lig fit protein which indicates that the ligand has diffused away from its original binding domain but stability was restored after 30–50 ns of simulation. The standard drug (benznidazole) showed large fluctuation and RMSD difference between the Cα and Lig fit Prot which was restored before the end of the simulation period (40–50 ns). The result of the RMSD plot (Fig. 5) revealed that the hit compounds

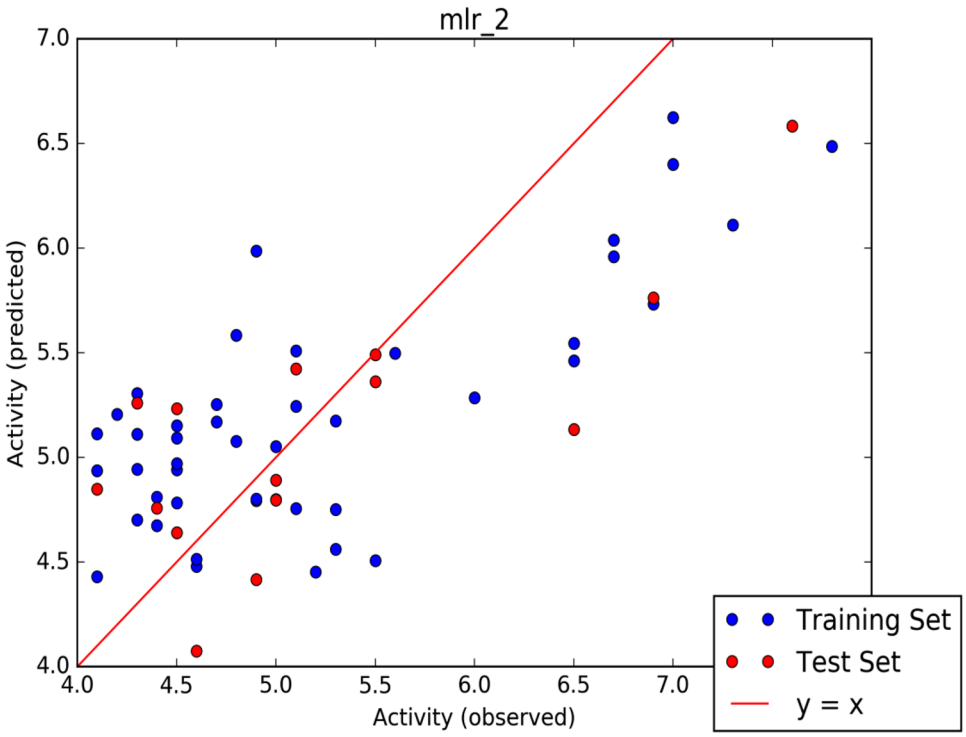

Fig. 4 Analysis of the scatter plot for the predictive model

Table 6 pIC_{50} of lead ligands using predictive model

ID	Compounds	pIC_{50} (μM)
15560423	Kulactone	4.513
65084	(+)(−)Gallocatechin	4.686
72276	(−)(−)Epicatechin	4.898
101761	Erythrodiol	3.897
5281605	Baicalein	4.726
72281	Hesperetin	4.594
5280445	Luteolin	4.958
4788	Phloretin	4.737
5280343	Quercetin	4.703
31593	Benznidazole (standard)	5.817

(kulactone and gallocatechin)-sterol-14-α-demethylase protease complexes are more stable with sight fluctuation compared with the benzidazole- sterol-14-α-demethylase protease complex.

3.6 Analysis of the Root Mean Square Fluctuation (RMSF)

The dynamic behavior of the amino acid of the ligand–protein complexes were evaluated by computing the atomic positional fluctuation of the amino acid backbone of the protein. Hence, the local changes along the sterol-14-α-demethylase residues were monitored by the RMSF value for

Table 7 Molecular properties obtained via DFT at the B3LYP/6-31G (d) level of theory

Compounds	E_{HOMO} (eV)	E_{LUMO} (eV)	E_g (eV)	I (eV)	A (eV)	η (eV)	δ (eV^{-1})	χ (eV)
Kulactone	−6.22	−0.43	5.79	6.22	0.43	2.895	0.3454	3.325
(−)-Gallocatechin	−5.65	0.02	5.67	5.65	−0.02	2.835	0.3527	2.815
(−)-Epicatechin	−5.55	0.14	5.69	5.55	−0.14	2.845	0.3515	2.705
Erythrodiol	−5.98	0.78	6.76	5.98	−0.78	3.38	0.2959	2.6
Hesperetin	−5.76	−1.38	4.38	5.76	1.38	2.19	0.4566	3.57
Luteolin	5.88	−1.76	−7.64	−5.88	1.76	−3.82	−0.2617	−2.06
Quercetin	−5.48	−1.84	3.64	5.48	1.84	1.82	0.5494	3.66
Phloretin	−5.62	−1.28	4.34	5.62	1.28	2.17	0.4608	3.45
Baicalein	−5.74	−1.89	3.85	5.74	1.89	1.925	0.5194	3.815
Benznidazole	−6.69	−2.76	3.93	6.69	2.76	1.695	0.5880	4.725

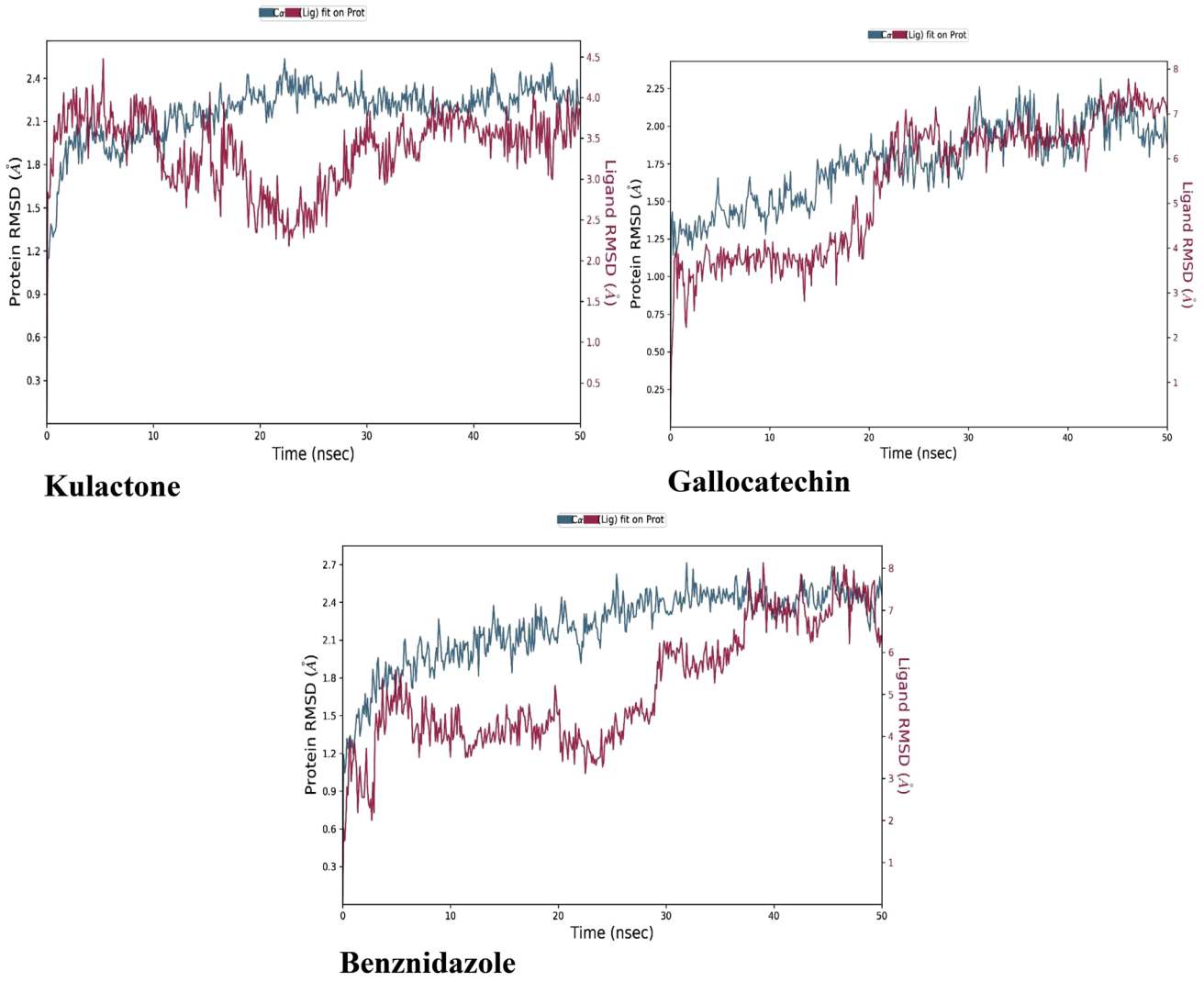

Fig. 5 RMSD calculation for Cα atoms (blue) sterol 14-demethylase protease and Ligands fit Protein (red) at 50 ns simulation period

50 ns simulation time. The α-helices and β-strands of sterol-14-α-demethylase structure were shown to oscillate within 1.0–2.5 Å for the hit compounds and standard ligand (benzidazole) (Fig. 6). The secondary parameters like β-strands and α-helices are more stable than the unstructured portion of the protein, and thus show less fluctuation than the loop regions. The loop regions of the sterol-14-α-demethylase in all the complexes revealed high fluctuation above 4.5 Å.

3.7 Interaction Mapping Between Protein–Ligand Complexes

The binding orientation of sterol-14-α-demethylase—ligand complexes established by docking model was further validated for stability of the intermolecular interaction, although simulation reveals the binding conformation by averaging all sterol-14-α-demethylase–ligand interactions obtained from individual frames of the trajectory and predicts the most favored contacts. From Fig. 7, all the docked compounds showed better interactions with amino acid in the selected site of sterol-14-α-demethylase structure during

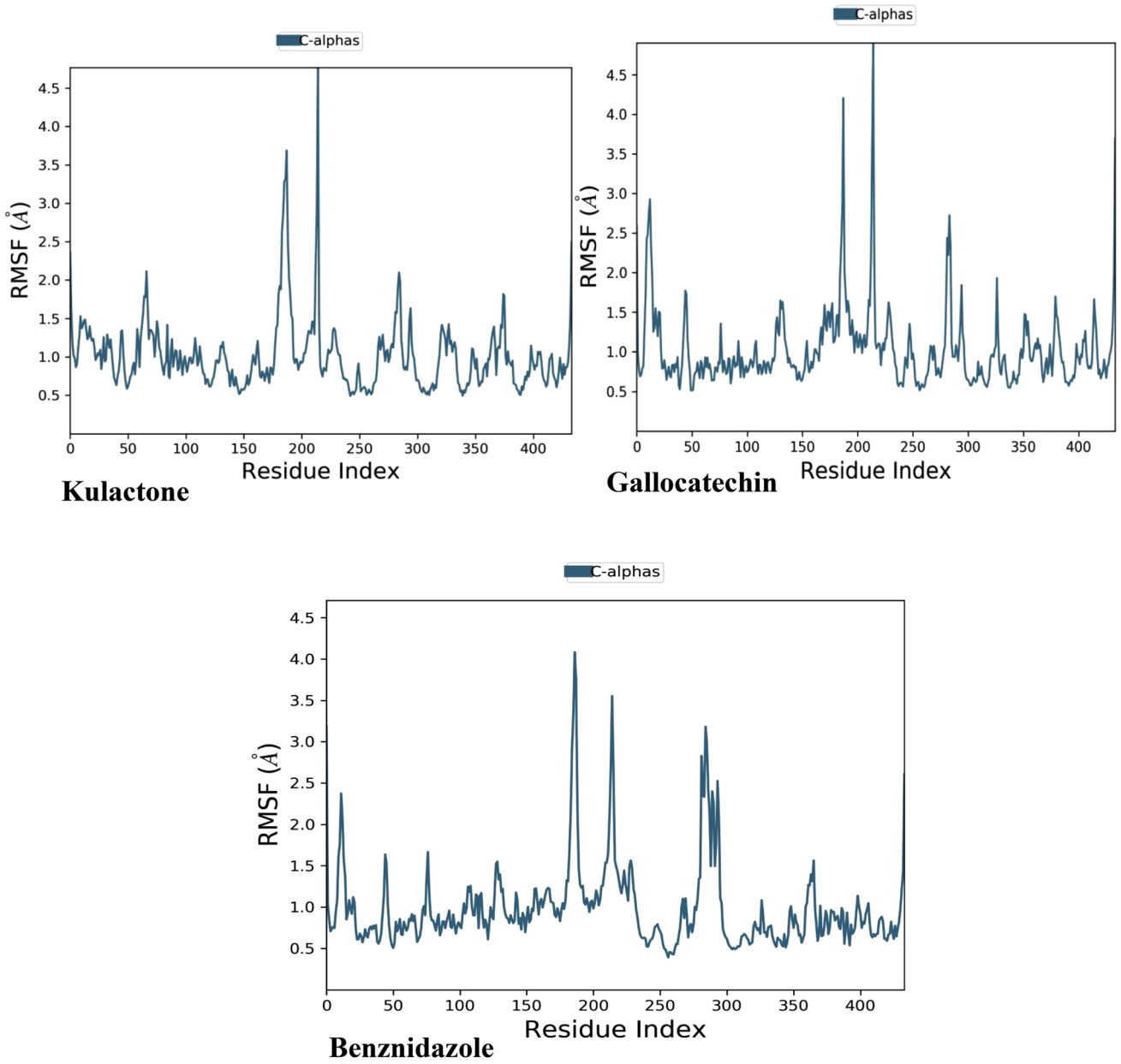

Fig. 6 Line representation of the evolution of root mean square fluctuation (RMSF) of sterol 14-demethylase protease Cα during 50 ns MD simulation

the simulation time. Interestingly, the ligands interacted with residues of the binding site of sterol-14-α-demethylase with hydrophobic bond, hydrogen bond and water bridges. Gallocatechin was shown to exhibits high H-bond interactions with vital amino acid residues in the binding site of sterol-14-α-demethylase at > 60% of the simulation interval compared to the standard drug. However, the hit compounds and benznidazole were observed to form H-bond interaction with ARG 361 with varying interaction fraction with kulactone forming above 1.2, gallocatechin forming 0.6 which are comparable to benznidazole (0.6). The standard drug was observed to exhibit more hydrophobic interaction with the amino acid of sterol-14-α-demethylase binding site.

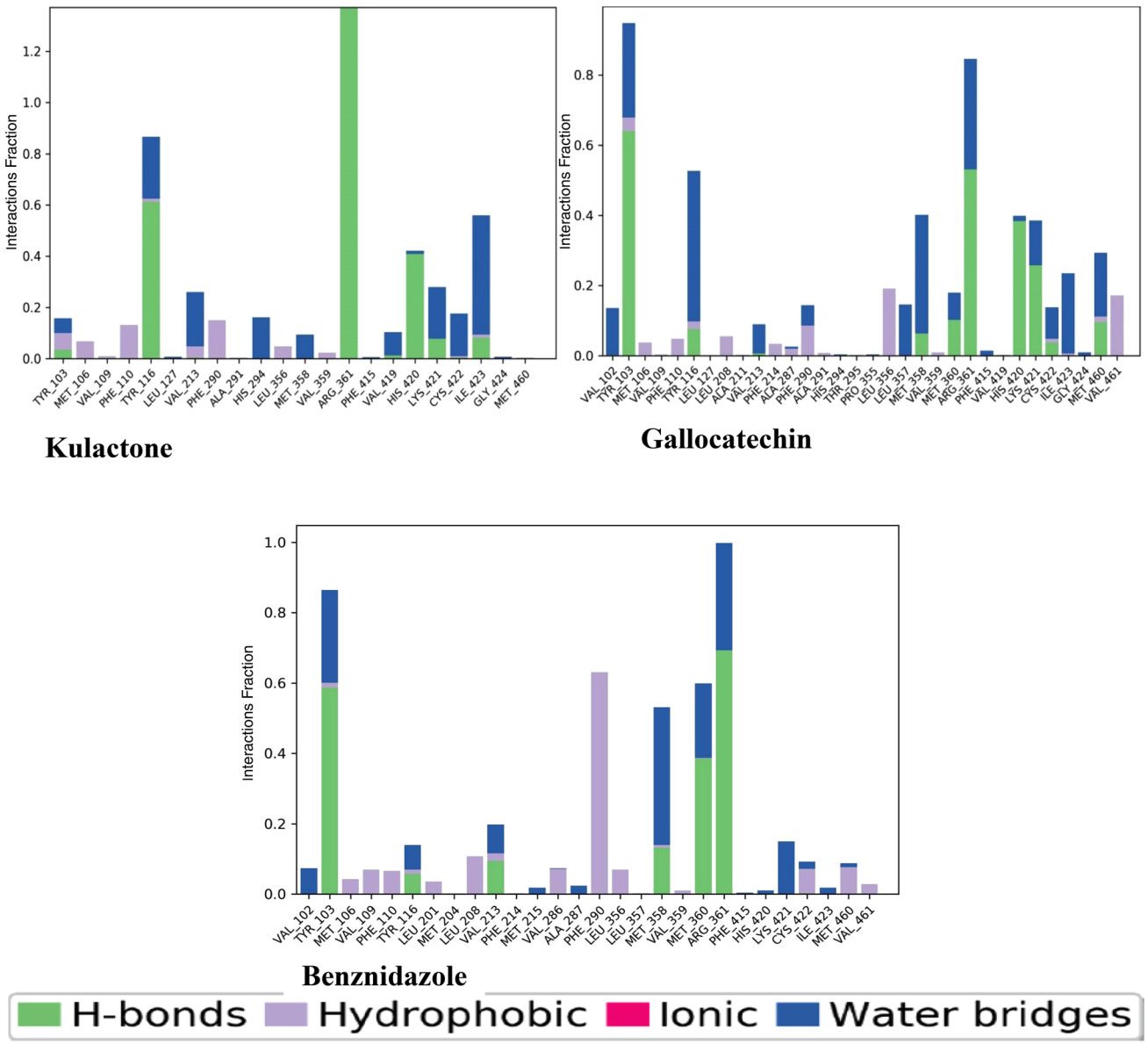

Fig. 7 Interaction of the protein–ligand mapping for sterol 14-demethylase protease

4 Conclusion

Sterol-14-α-demethylase is a key therapeutic target which has been identified in drug design and development against chagas disease. This study was performed to predict potent antagonists of sterol-14-α-demethylase from *Ilex kudingcha* compounds which can block the active site of the protein by employing computational models. Molecular docking, MM/GBSA calculation, quantum chemical calculation and virtual ADME screening of the molecules were carried out followed by MD simulation studies of hit compounds-sterol-14-α-demethylase complexes. The analysis predicted nine (9) lead compounds from the post-docking studies. Two top scored complexes were further validated by subjecting them to MD simulation study. Kulactone and gallocatechin satisfied all the parameters investigated including the MD simulation analysis. Therefore, these two compounds (kulactone and gallocatechin) were predicted as inhibitors of sterol-14-α-demethylase. However, further validation of our findings experimental analysis is suggested to establish the efficacy of the predicted compounds as drug candidate in the management of chagas disease.

Supplementary Information The online version contains supplementary material available at https://doi.org/10.1007/s42250-022-00565-4.

Data availability The research data associated with this paper is available, it can be accessible on request from the authors.

References

1. Omoboyowa DA (2022) Exploring molecular docking with E-pharmacophore and QSAR models to predict potent inhibitors of 14-α-demethylase protease from *Moringa* spp. Pharmacol Res-Modern Chin Med 4:100147. https://doi.org/10.1016/j.prmcm.2022.100147
2. Lidani KCF, Andrade FA, Bavia L, Damasceno FS, Beltrame MH, Messias-Reason IJ, Sandri TL (2019) Chagas disease: from discovery to a worldwide health problem. Front Public Health 7:166. https://doi.org/10.3389/fpubh.2019.00166
3. Conlan J, Lal A (2015) Socioeconomic burden of foodborne parasites. In: Gajadhar AA (ed) Woodhead Publishing Series in food science, technology and nutrition, foodborne parasites in the food supply web. Woodhead Publishing, pp 75–98. https://doi.org/10.1016/B978-1-78242-332-4.00005-9
4. Ribeiro A, Nunes M, Teixeira M (2012) Diagnosis and management of Chagas disease and cardiomyopathy. Nat Rev Cardiol 9:576–589. https://doi.org/10.1038/nrcardio.2012109
5. Buckner FS (2008) Sterol 14-demethylase inhibitors for trypanosoma cruzi infections. Drug targets in kinetoplastid parasites. Springer, pp 61–80
6. Antas PR, Medrano-Mercado N, Torrico F, Ugarte-Fernandez R, Gómez F, Correa Oliveira R, Chaves AC, Romanha AJ, Araújo-Jorge TC (1999) Early, intermediate, and late acute stages in Chagas' disease: a study combining anti-galactose IgG, specific serodiagnosis, and polymerase chain reaction analysis. Am J Trop Med Hyg 61(2):308–314. https://doi.org/10.4269/ajtmh.1999.61.308
7. Andrade DV, Gollob KJ, Dutra WO (2014) Acute chagas disease: new global challenges for an old neglected disease. PLoS Negl Trop Dis 8(7):e3010. https://doi.org/10.1371/journal.pntd.0003010
8. Pinheiro E, Brum-Soates L, Reis R, Cubides J (2017) Chagas disease: review of needs, neglect, and obstacles to treatment access in Latin America. Rev Soc Bras Med Trop 50(3):296–300. https://doi.org/10.1590/0037-8682-0433-2016
9. Lepesheva GI, Villalta F, Waterman MR (2011) Targeting *Trypanosoma cruzi* sterol 14α-demethylase (CYP51). Adv Parasitol 5:65–87. https://doi.org/10.1016/B978-0-12-385863-4.00004-6
10. Fabricant DS, Farnsworth NR (2001) The value of plants used in traditional medicine for drug discovery. Environ Health Perspect 109(Suppl 1):69–75
11. Li L, Xu LJ, Ma GZ, Dong YM, Peng Y, Xiao PG (2013) The large-leaved Kudingcha (*Ilex latifolia* Thunb and *Ilex kudingcha* C.J. Tseng): a traditional Chinese tea with plentiful secondary metabolites and potential biological activities. J Nat Med 67(3):425–437. https://doi.org/10.1007/s11418-013-0758-z
12. Sun Y, Xu W, Zhang W, Hu Q, Zeng X (2011) Optimizing the extraction of phenolic antioxidants from kudingcha made from *Ilex kudingcha* C.J. Tseng by using response surface methodology. Sep Sci Technol 78:311–320
13. Soniran O, Ngele K, Onyemeziri CA, Omoboyowa DA, Nnabude A (2018) Histopathological studies on the effects of chloroform and methanolic extracts of *Ilex kudingcha* in *Trypanosoma brucei* infected Albino Wistar Rats. Recent Adv Biol Med. 4:50–62. https://doi.org/10.18639/RABM.2018.04.735155
14. Omoboyowa DA (2022) Virtual screening of phyto-compounds from *Blighia sapida* as protein tyrosine phosphatase 1B inhibitor: a computational approach against diabetes. Chem Afr 5:1–11. https://doi.org/10.1007/s42250-022-00373-w
15. Omoboyowa DA, Iqbal MN, Balogun TA, Bodun DS, Fatoki JO, Oyeneyin OE (2022) Inhibitory potential of phytochemicals from Chromolaema odorata L against apoptosis signal-regulatory kinase 1: a computational model against colorectal cancer. Comput Toxicol 23:100235
16. Ferreira L, Dos Santos R, Oliva G, Andricopulo A (2015) Molecular docking and structure-based drug design strategies. Molecules 20(7):13384–13421. https://doi.org/10.3390/molecules200713384
17. Omoboyowa DA, Singh G, Fatoki JO, Oyeneyin OE (2022) Computational investiga-tion of phytochemicals from *Abrus precatorius* seeds as modulators of peroxisome proliferator-activated receptor gamma (PPAR γ). J Biomol Struct Dyn 40:1–16. https://doi.org/10.1080/07391102.2022.2091657
18. Kitchen D, Decornez H, Furr J, Bajorath J (2004) Docking and scoring in virtual screening for drug discovery: methods and applications. Nat Rev Drug Discov. 3(11): 935–949. https://www.nature.com/articles/nrd1549
19. Pace NJ, Weerapana E (2013) Diverse functional roles of reactive cysteines. ACS Chem Biol 8:283–296
20. Barford D (2004) The role of cysteine residues as redox-sensitive regulatory switches. Curr Opin Struct Biol 14:679–686
21. Maurias AJ, Weerapana E (2019) Reactive-cysteine profiling for drug discovery. Curr Opin Chem Biol 50:29–36
22. Genheden S, Ryde U (2015) The MM/PBSA and MM/GBSA methods to estimate ligand-binding affinities. Expert Opin Drug Discov 10(5):449–461
23. Ritchie TJ, Macdonald SJF, Peace S, Pickett SD, Luscombe CN (2013) Increasing small molecule drug developability in suboptimal chemical space. Med Chem Commun 4:673–680
24. Lipinski CA, Lombardo F, Dominy BW, Feeney PJ (2001) Experimental and computational approaches to estimate solubility and permeability in drug discovery and development settings. Adv Drug Deliv Rev 46:3–26
25. Margulis E, Dagan-Wiener A, Ives RS, Jaffari S, Siems K, Niv MY (2021) Intense bitterness of molecules: machine learning for expediting drug discovery. Comput Struct Biotechnol J 19:568–576
26. Ghose AK, Herbertz T, Hudkins RL, Dorsey BD, Mallamo JP (2012) Knowledge-based, central nervous system (CNS) lead selection and lead optimization for CNS drug discovery. ACS Chem Neurosci 3(1):50–68
27. Van-Breemen RB, Li Y (2005) Caco-2 cell permeability assays to measure drug absorption. Expert Opin Drug Metab Toxicol 1(2):175–185
28. Jin X, Luong TL, Reese N, Gaona HV, Collazo-Velez C, Vuong B, Potter JC, Sousa R, Olmeda Q, Li L, Xie J, Zhang P, Zhang G, Reichard V, Melendez SR, Marcsisin BS (2014) Pybus, comparison of MDCK-MDR1 and Caco-2 cell based permeability assays for anti-malarial drug screening and drug investigations. J Pharmacol Toxicol Methods 70(2):188–194. https://doi.org/10.1016/j.vascn.2014.08.002
29. Kwon S, Bae H, Jo J (2019) Comprehensive ensemble in QSAR prediction for drug discovery. BMC Bioinform 20:521. https://doi.org/10.1186/s12859-019-3135-4
30. Ponmary PLD, Jeya SSD (2010) QSAR study for the prediction of IC_{50} and logP for 5-*N*-acetyl-beta-D-neuraminic acid structurally similar compounds using stepwise (multivariate linear regression. Int J Chem Res 2(1):32–38
31. Tandon H, Chakraborty T, Suhang V (2019) A brief review on importance of DFT in drug design. Res Med Eng Sci 7(4):791–795

32. Uzzaman MT, Mahmud T (2020) Structural modification of aspirin to design new potential cyclooxygenase (COX-2) inhibitors. In Silico Pharmacol 8:1
33. Balogun TA, Iqbal MN, Saibu OA, Akintubosun MO, Lateef OM, Nneka UC, Abdullateef OT, Omoboyowa DA (2021) Discovery of potential HER2 inhibitors from *Mangifera indica* for the treatment of HER2-Positive breast cancer: an integrated computational approach. J Biomol Struct Dyn 39:1–12
34. Baell JB, Congreve M, Leeson P, Abad-Zapatero C (2013) Ask the experts: past, present and future of the rule of five. Fut Med Chem 5:745–752